Temperature dependence of the anisotropic magnetic penetration depth and lower critical field of single-crystal $Pb_2Sr_2(Y,Ca)Cu_3O_{8+\delta}$

M. Reedyk, C. V. Stager, and T. Timusk
Department of Physics, McMaster University, Hamilton, Ontario, Canada L8S 4M1

J. S. Xue and J. E. Greedan
Institute for Materials Research, McMaster University, Hamilton, Ontario, Canada L8S 4M1
(Received 15 August 1990; revised manuscript received 25 February 1991)

The temperature dependence of the penetration depth of single-crystal $Pb_2Sr_2(Y,Ca)Cu_3O_{8+\delta}$ has been determined in the vicinity of T_c ($\sim$75 K) using intermediate-field reversible-magnetization measurements. The *ab*-plane penetration depth in the restricted region near T_c was found to follow clean-limit BCS behavior from which an estimate of 2575 Å for $\lambda_{ab}(0)$ was obtained. The effective-mass anisotropy parameter, $\gamma=(m_c/m_{ab})^{1/2}$, was found to be 2.5, which together with the former result yields a value of 6425 Å for $\lambda_c(0)$. In addition, the temperature dependence of the anisotropic lower critical field was determined from observations of the onset of deviation from perfect diamagnetism. The estimates obtained for the zero-temperature lower critical field, $H_{c1}(0)$, were 95±10 G for $\mathbf{H}\perp c$ and 505±20 G for $\mathbf{H}\parallel c$.

I. INTRODUCTION

One of the most notable aspects of the cuprate oxide high-temperature superconductors is their highly anisotropic structure and the implications that this has for their physical properties. To date, the most thoroughly investigated member of this family is $YBa_2Cu_3O_{7-\delta}$, although many studies of $Bi_2Sr_2CaCu_2O_8$, which contains similar CuO_5 pyramidal bilayers, have also been undertaken. It is recognized that the differences in the behavior of various physical properties of these systems may stem from the layers between successive CuO_2 bilayers: the CuO chains in $YBa_2Cu_3O_{7-\delta}$ and the double BiO sheets in $Bi_2Sr_2CaCu_2O_8$. The anistropy between *ab*-plane and *c*-axis properties of $Bi_2Sr_2CaCu_2O_8$ has been found to be much larger than in $YBa_2Cu_3O_{7-\delta}$,[1] which is attributed in part to the larger interlayer spacing in $Bi_2Sr_2CaCu_2O_8$ (12 Å between successive double CuO_2 plane layers as compared to 8 Å in $YBa_2Cu_3O_{7-\delta}$), leading to more "quasi"-two-dimensional behavior. Although it is not yet well appreciated, $Pb_2Sr_2(Y,Ca)Cu_3O_{8+\delta}$ is a third structurally distinct, as opposed to $Tl_2Ba_2CaCu_2O_8$, which is to a first approximation isostructural with $Bi_2Sr_2CaCu_2O_8$, cuprate oxide superconductor containing CuO_2 plane bilayers.[2] $Pb_2Sr_2(Y,Ca)Cu_3O_{8+\delta}$ is interesting from the point of view of comparison with the other two materials because its intercalary structure contains elements in common with both systems. In $Pb_2Sr_2(Y,Ca)Cu_3O_{8+\delta}$ the double CuO_2 plane layers are separated by a PbO-CuO_δ-PbO sequence, the two PbO layers being analogous to the double BiO sheets in $Bi_2Sr_2CaCu_2O_8$ and the CuO_δ layer comparable to an oxygen-depleted chain layer such as in $YBa_2Cu_3O_6$. In addition, the interlayer spacing in $Pb_2Sr_2(Y,Ca)Cu_3O_{8+\delta}$ is 12.3 Å, very close to that in $Bi_2Sr_2CaCu_2O_8$.

$Pb_2Sr_2(Y,Ca)Cu_3O_{8+\delta}$ is the only superconducting member of the Pb-cuprate family available in single-crystal form, thus enabling investigations of anisotropy. It is therefore fitting to begin a study of the physical properties of this system to establish its relation to the other materials. In particular, it is of interest to determine the extent of the anisotropy in this system in comparison with the other two.

It is likely that the CuO chain layer in $YBa_2Cu_3O_{7-\delta}$ provides some electronic coupling between successive CuO plane bilayers which is absent in $Bi_2Sr_2CaCu_2O_8$. Since $Pb_2Sr_2(Y,Ca)Cu_3O_{8+\delta}$ contains, in addition to the PbO sheets, an interlayer of Cu, one might therefore expect the anisotropy in this system to be intermediate to that in the other two. We report herein on low- and intermediate-field magnetization measurements of $Pb_2Sr_2(Y,Ca)Cu_3O_{8+\delta}$, which, through determination of the anisotropy between the *ab*-plane and *c*-axis penetration depth and lower critical field, makes a start toward addressing these concerns.

II. SAMPLE CHARACTERIZATION

A detailed general characterization of our $Pb_2Sr_2(Y,Ca)Cu_3O_{8+\delta}$ crystals, synthesized using a PbO-NaCl flux method, via the Guinier powder technique, single-crystal x-ray diffraction, electron diffraction, neutron activation analysis, mass spectrometry, thermogravimetric analysis (TGA), energy-dispersion x-ray (EDX) analysis, and dc resistivity and magnetization has already been reported.[3] The crystal utilized in this study (approximate dimensions $0.7\times0.6\times0.2$ mm^3) was annealed in a nitrogen atmosphere at 600 °C for 40 h, a procedure that has been found to improve the sharpness of the magnetically measured transition and extend the range over which the magnetization is reversible. Single-crystal x-ray analysis of this particular crystal using the Weissen-

berg technique showed it to be of good crystal quality [all of the reflections in the Weissenberg photograph can be indexed to a primitive orthorhombic unit cell of $a=5.383(1)$ Å, $b=5.423(1)$ Å, and $c=15.765(2)$ Å, implying that there is no evidence of any secondary phase]. EDX analysis of four randomly chosen locations on the surface of the crystal showed that compositional differences in Pb, Sr, Ca, and Y, as deduced from the ratio of the measured intensity of the Pb $M\alpha$, and Sr, Ca, and Y $K\alpha$ radiation to the Cu $K\alpha$ were less than 2% in all cases, except for Sr, where a maximum of 3% difference was observed. The variation in the magnitude of the Cu $K\alpha$ signal itself was no more than 3%. These results show that the crystal is of good homogeneity in composition.

III. ANISOTROPIC MAGNETIC PENETRATION DEPTH

It is well established that for fields between the lower and upper critical fields $H_{c1} \ll H \ll H_{c2}$, the reversible magnetization of an isotropic type-II superconductor varies as $\ln H$ according to[4]

$$M=\frac{H_{c1}}{8\pi \ln(\lambda/\xi)}\ln\left[\frac{H}{H_{c2}\beta}\right], \tag{1}$$

where λ and ξ are the magnetic penetration depth and coherence length, respectively, and β is a constant which depends on a cutoff, chosen to overcome an unphysical logarithmic singularity in evaluating an integral approximation to a sum over the reciprocal vortex lattice (and therefore also on the form of the lattice). With H_{c1} given by the approximate London formula[4]

$$H_{c1}=\frac{\Phi}{4\pi\lambda^2}\left[\ln\left[\frac{\lambda}{\xi}\right]+0.5\right], \tag{2}$$

where $\Phi=2.07\times10^{-7}$ G cm^2 is the flux quantum, and the additive factor of 0.5 is neglected in the high $\kappa=\lambda/\xi$ limit, Eq. (1) becomes

$$M=\frac{\Phi}{32\pi^2\lambda^2}\ln\left[\frac{H}{H_{c2}\beta}\right]. \tag{3}$$

Kogan, Fang, and Mitra have extended this analysis to include electronic anisotropy by replacing the isotropic penetration depth λ by a tensor.[5] Neglecting distinctions between the a and b directions, the magnetization for the c axis of the crystal oriented parallel or perpendicular to the field direction is then given by

$$\begin{aligned} M_{\|c}&=\frac{\Phi}{32\pi^2\lambda_{ab}^2}\ln\left[\frac{H}{H_{c2}^{\|}\beta}\right], \\ M_{\perp c}&=\frac{\Phi}{32\pi^2\lambda_{ab}\lambda_c}\ln\left[\frac{H}{H_{c2}^{\perp}\beta}\right], \end{aligned} \tag{4}$$

respectively, where λ_{ab} is the ab-plane penetration depth and λ_c the penetration depth along the c direction. A plot of $M_{\|c}$ as a function of $\ln H$ will therefore have slope $dM_{\|c}/d\ln H=\Phi/32\pi^2\lambda_{ab}^2$. It is clear that the temperature dependence of the ab-plane penetration depth may then be extracted by evaluating this quantity at several different temperatures. Similarly, once $\lambda_{ab}(T)$ is known, the experimental slope values $dM_{\perp c}/d\ln H=\Phi/32\pi^2\lambda_{ab}\lambda_c$ can be used to determine the temperature dependence of the c-axis penetration depth. In general, λ^{-2} is expected to vary linearly with temperature in the vicinity of T_c[4] so that a plot of $dM/d\ln H$ as a function of temperature should be linear near T_c. Furthermore, from (4), the ratio of $dM_{\|c}/d\ln H$ to $dM_{\perp c}/d\ln H$ yields λ_c/λ_{ab}, which, since λ^2 is proportional to the effective mass,[4] m, is equal to the effective-mass anisotropy parameter $\gamma=(m_c/m_{ab})^{1/2}$ used to characterize the extent of the anisotropy in the system. Thus, since $dM/d\ln H$ is linear in temperature near T_c, γ can be obtained from the ratio of the slopes corresponding to the two field orientations:

$$\gamma=\frac{d}{dT}\left[\frac{dM_{\|c}}{d\ln H}\right]\Big/\frac{d}{dT}\left[\frac{dM_{\perp c}}{d\ln H}\right]. \tag{5}$$

In (4), $H_{c2}^{\|}$ and $H_{c2}^{\perp}$ refer to the value of the upper critical field when the applied field is parallel and perpendicular to the c axis of the crystal, respectively. Although the anisotropy in H_{c2} has been written explicitly, the present analysis is unaffected since it is based on the slope of the $M(\ln H)$ curve, which is independent of H_{c2}.

A. Experiment

The crystal of $Pb_2Sr_2(Y,Ca)Cu_3O_{8+\delta}$ was mounted on a quartz rod and placed into a Quantum Design superconducting quantum interference device (SQUID) magnetometer with its c axis oriented either perpendicular or parallel to the field direction. For each orientation the magnetization was measured as a function of temperature in the vicinity of T_c ($\sim$75 K) for magnetic fields of 0.1, 0.4, 0.7, and 1.0–5.5 T in steps of 0.5 T. Generally, the field was turned on after a zero-field cool to 55 K and the resulting magnetization measured upon warming, although some field-cooled sequences were performed in order to determine the regime of reversible magnetization, as discussed below.

B. Results

Several of the resulting curves, with a background diamagnetic moment that is temperature independent and linear in field subtracted, are shown in Fig. 1(a) and 1(b) for the c axis of the crystal oriented perpendicular and parallel to the magnetic field, respectively. In Fig. 1(a), since the magnetization is close to an order of magnitude smaller and hence has a much lower signal-to-noise ratio than that for $\mathbf{H}\|c$, we show for clarity only curves for three magnetic-field strengths. Although the temperature range shown constitutes in all cases the region in which the magnetization was found to be reversible, we show in the inset to Fig. 1(b) both field- and zero-field-cooled results for $\mathbf{H}\|c$ for magnetic-field strengths of 1.0 and 5.0 T in order to illustrate the extent of the reversible magnetization. The region of reversibility is smaller for

H perpendicular to c than for **H** parallel to c.

The magnetization data were then replotted as a function of $\ln H$ for temperatures in the reversible regime in 0.5-K steps. Some representative results are shown in Figs. 2(a) and 2(b) for **H** perpendicular and parallel to c, respectively. The expected linear behavior is seen clearly for **H** parallel to c. Because of the much smaller signal-to-noise ratio in the $\mathbf{H}\perp c$ data, the linearity is less obvious. Proceeding, nevertheless, with the analysis, Fig. 3 shows the temperature dependence of the least-squares determined slopes of the $M(\ln H)$ curves. Note that for both orientations the linear behavior expected near T_c is present, which provides an *a posteriori* justification for the use of the $\mathbf{H}\perp c$ data.

The effective-mass anisotropy parameter γ can be determined from the ratio of the least-squares slopes of the two curves in Fig. 3 according to Eq. (5). The result is $\gamma = 2.5$ or $m_c/m_{ab} = \gamma^2 \approx 6$.

Figure 4(a) shows the temperature dependence of λ_{ab} and λ_c calculated as discussed above. Of primary interest is the zero-temperature penetration depth. From the restricted temperature range investigated, it is difficult to extract $\lambda(0)$, although an estimate is possible by comparing the experimental results with the expected behavior for various models. The usual procedure is to plot $[\lambda(0)/\lambda(T)]^2$ as a function of reduced temperature T/T_c. The fitting parameters are then $\lambda(0)$ and T_c. Note, however, that T_c can be discerned directly from Fig. 3 since, at T_c, $dM/d\ln H$ is zero. Comparable values are found for the two orientations, 74.7 K for **H** parallel to c and

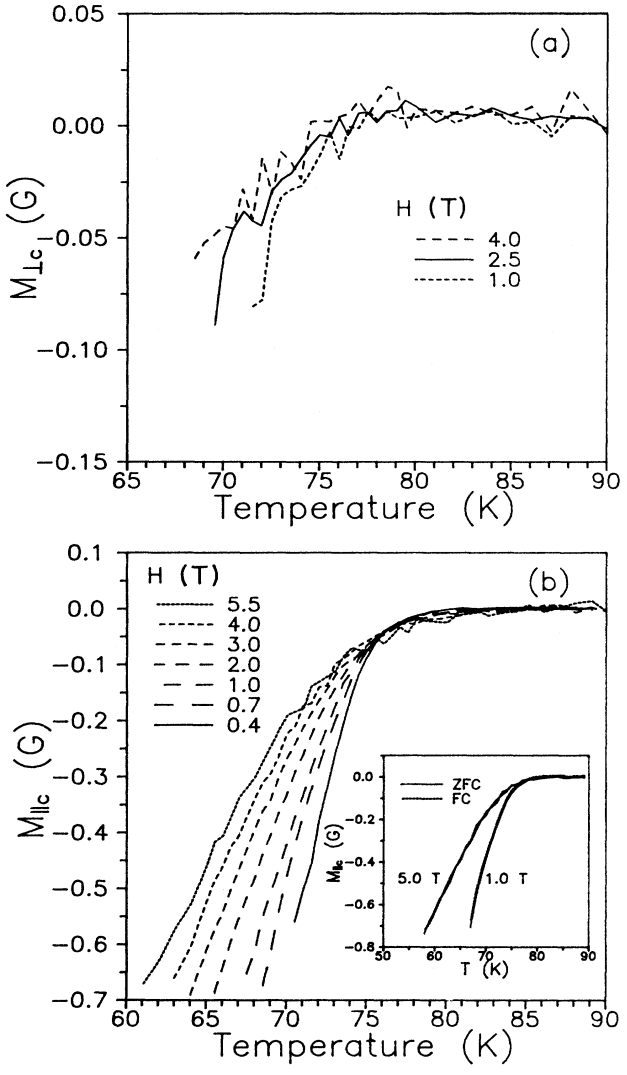

FIG. 1. Temperature dependence of the magnetization of $Pb_2Sr_2(Y,Ca)Cu_3O_{8+\delta}$ at various magnetic-field strengths for the c axis of the crystal oriented (a) perpendicular ($M_{\perp c}$) and (b) parallel ($M_{\parallel c}$) to the field direction. Inset to (b): Field-cooled (FC) and zero-field-cooled (ZFC) curves to illustrate the extent of the reversibility of $M_{\parallel c}$.

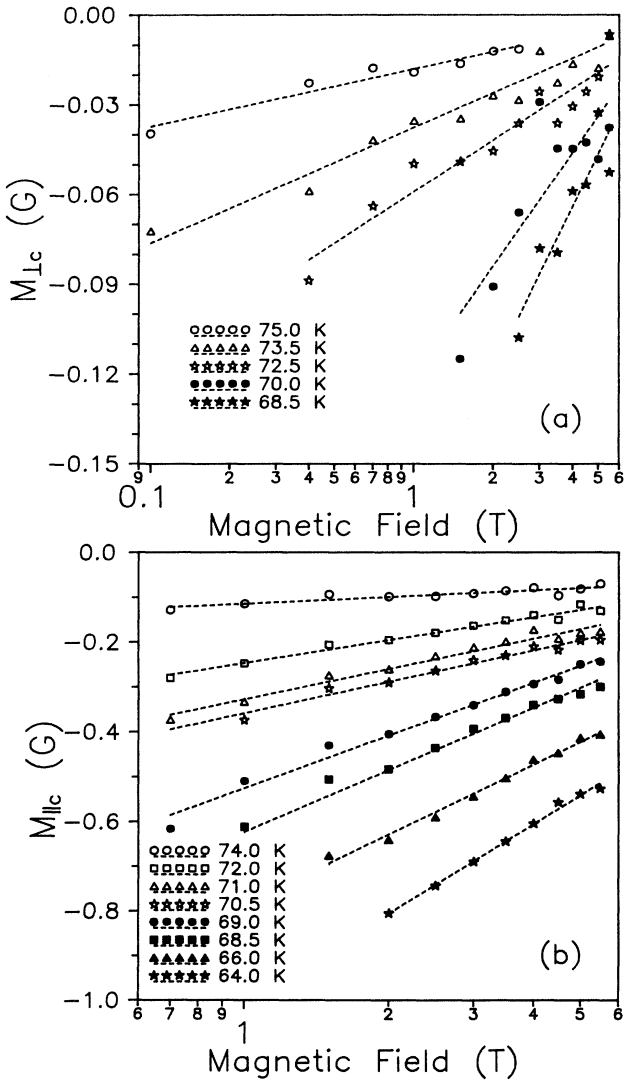

FIG. 2. Magnetic-field dependence of the magnetization of $Pb_2Sr_2(Y,Ca)Cu_3O_{8+\delta}$ at various temperatures for (a) $\mathbf{H}\perp c$ and (b) $\mathbf{H}\parallel c$. The dashed curves represent least-squares fits to the data.

75.3 K for **H** perpendicular to c. These values correspond closely to the 90% criterion for determining T_c from the low-field magnetic transition measured with a small negative field ($-1 < H < 0$ G) and shown in the inset to the figure.

In Fig. 4(b) we show the best fit of the ab-plane data [fitting parameter $\lambda_{ab}(0)$ with $T_c = 74.7$ K] to the prediction for $[\lambda(0)/\lambda(T)]^2$ for the two-fluid model and in the BCS dirty and clean (or London) limits. In this restricted temperature range, the data appear to be described better by BCS than by two-fluid behavior [i.e., if as has been done in Fig. 4(b), $\lambda(0)$ is chosen such that the data points follow the two-fluid behavior near T_c, then the data points at lower temperature fall significantly above the theoretical curve, whereas in the BCS cases a value can be chosen for $\lambda(0)$ such that the data points follow the theoretical behavior reasonably well throughout the range of temperatures investigated]. The scatter in the data is such that it is difficult to distinguish between dirty and clean-limit BCS behavior. We thus conclude simply that from the fit to BCS clean-limit behavior we obtain a lower limit for $\lambda_{ab}(0)$ of 2575 Å. The c-axis penetration depth data are more scattered and limited in extent, and thus rather than predict $\lambda_c(0)$ by fitting to theory, we make use of the experimentally determined effective-mass anisotropy. With $\lambda_{ab}(0)$ given by the BCS clean-limit result (2575 Å) and $\lambda_c(0)/\lambda_{ab}(0) = (m_c/m_{ab})^{1/2} = 2.5$, we obtain 6425 Å for $\lambda_c(0)$.

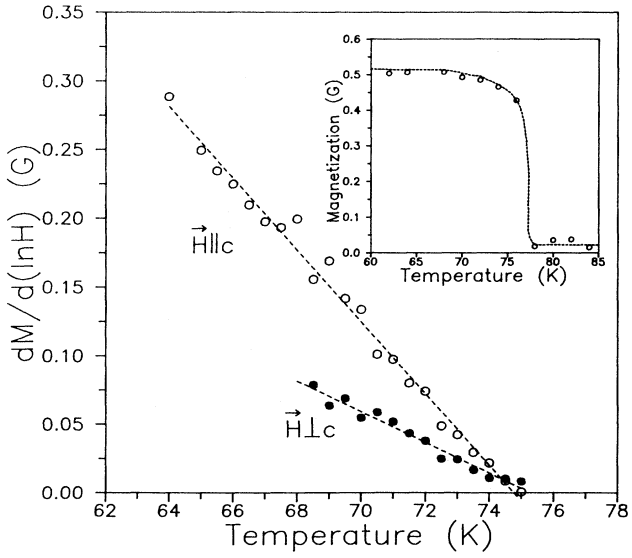

FIG. 3. Temperature dependence of $dM/d(\ln H)$ for the two crystal orientations of interest. Note the expected linear behavior. The dashed curves represent least-squares fits to the data. The ratio of the slopes gives the anisotropy parameter $\gamma = (m_c/m_{ab})^{1/2} \approx 2.5$. The horizontal intercept gives T_c. Note that the value obtained (~ 75 K) corresponds to the 90% saturation value of the low-field ($-1 < H < 0$ G) FC magnetic transition shown for $H \| c$ in the inset.

IV. ANISOTROPIC LOWER CRITICAL FIELD

It is now generally agreed that $\lambda_{ab}(0)$ for $YBa_2Cu_3O_{7-\delta}$ is of the order 1500 Å (values typically range from 1300 to 1700 Å).[6] Recent measurements for $Tl_2Ba_2CaCu_2O_8$ films yield a value of 2000 Å for $\lambda_{ab}(0)$,[7] while for single-crystal $Bi_2Sr_2CaCu_2O_8$, $\lambda_{ab}(0)$ has been found to be 3000 Å.[8] Mitra *et al.* point out that, according to Eq. (2), for $\lambda_{ab}(0)$ to be 3000 Å one would expect H_{c1} to be approximately 4 times smaller in $Bi_2Sr_2CaCu_2O_8$ than in $YBa_2Cu_3O_{7-\delta}$ since the coher-

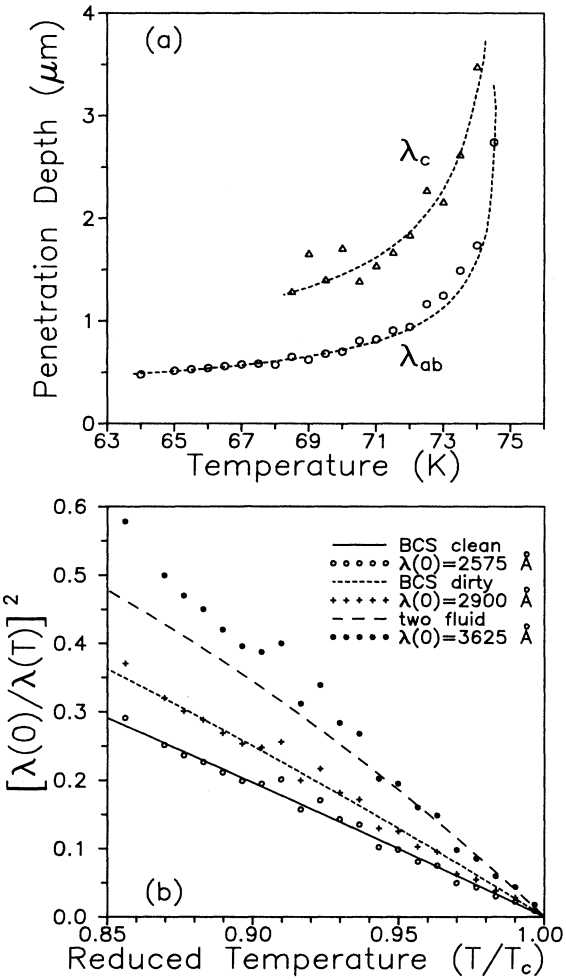

FIG. 4. Temperature dependence of the penetration depth of $Pb_2Sr_2(Y,Ca)Cu_3O_{8+\delta}$. (a) Absolute determination of λ_{ab} and λ_c in the vicinity of T_c. The dashed curves are a guide to the eye. (b) Fit of $[\lambda(0)/\lambda_{ab}(T)]^2$ vs T/T_c (points) to theory (curves). While it is clear that the data are less well described by the two-fluid curve (for which we have optimized the fit near T_c, yielding a clear deviation at lower temperatures), it is difficult to distinguish between the clean and dirty-limit BCS results since reasonable agreement can be obtained within the range of temperatures investigated in both cases. The BCS clean-limit fit yields a lower limit for $\lambda_{ab}(0)$ of 2575 Å.

ence lengths in $Bi_2Sr_2CaCu_2O_8$ are presumably of the same order of magnitude as in $YBa_2Cu_3O_{7-\delta}$. This reduction in H_{c1} should then also manifest itself to a somewhat smaller extent in $Pb_2Sr_2(Y,Ca)Cu_3O_{8+\delta}$. To address this matter we have attempted to estimate H_{c1} at low temperature following a method utilized by Naito *et al.* for $La_{2-x}Sr_xCuO_{4-\delta}$.[9]

H_{c1} is customarily determined from the low-field $M(H)$ curve as the field at which the onset of deviation from perfect diamagnetism is observed. This is, however, difficult to establish accurately in the cuprate oxide superconductors at low temperatures because the flux is heavily pinned and inhibited from entering the sample, giving rise to an almost undetectable deviation from perfect diamagnetism at H_{c1}. Natio *et al.* have circumvented this difficulty by using a procedure which yields a more pronounced anomaly at H_{c1}, thereby making it easier and less ambiguous to determine.

By definition, for $H \leq H_{c1}$, the equilibrium flux density $B = H + 4\pi M$ is zero so that M varies linearly with H. For $H > H_{c1}$, $H + 4\pi M (\equiv 4\pi \Delta M)$ is a quantity corresponding to the deviation of $M(H)$ from perfect diamagnetism. In Bean's critical-state model,[10] the equilibrium flux density for a slab of thickness D in a field parallel to its surface for $H \geq H_{c1}$ (and less than H^*, the field at which the flux fronts meet at the center of the sample) is given by

$$B(H_{c1} \leq H \leq H^*) = F(J_c, D)(H + 4\pi M)^{1/2} , \quad (6)$$

where $F(J_c,D)$ is a constant dependent on the critical-current density and dimensions of the sample. Naito *et al.* point out that since B $(H_{c1} \leq H \leq H^*)$ is directly proportional to $(\Delta M)^{1/2}$ a plot of $(\Delta M)^{1/2}$ as a function of applied magnetic-field strength should yield the equilibrium B-H curve. That is, $(\Delta M)^{1/2}$ should be zero until H reaches H_{c1}, whereupon it should begin to rise linearly with increasing field.

A. Experiment

For the determination of H_{c1}, isothermal-field-dependent magnetization measurements were carried out for both crystal orientations ($\mathbf{H} \| c$ and $\mathbf{H} \perp c$) at various temperatures. ΔM was then determined by fitting a straight line to the very-low-field $M(H)$ data and subsequently subtracting this least-squares fit from the full data set.

B. Results

Figure 5(a) show the low-field $M(H)$ data obtained at 5 K for the c axis of the crystal oriented both perpendicular and parallel (inset) to the direction of the applied field together with a least-squares fit to the very-low-field regime. Note that the slopes are very different in the two cases. This is due to demagnetization, the effect being, as expected, less severe for $\mathbf{H} \perp c$ than for $\mathbf{H} \| c$ as a result of the platelike geometry of the sample (the c axis being as usual the smallest dimension). We have measured many crystals of different shapes and sizes, made approximations to the geometry in order to estimate the demagnetization factor for $\mathbf{H} \| c$,[11] and in each case find that the volume fraction of superconducting material is within 10% or less of 100%, from which we conclude that we have essentially complete diamagnetic shielding in our crystals. The most straightforward solution to the problem of accounting for this effect is then to assume perfect shielding at low fields, which together with the measured slope dM/dH determines the demagnetization factor.

The demagnetization factors calculated in this manner are $N_{\|} = 0.64$ and $N_{\perp} = 0.14$ for $H \| c$ and $\mathbf{H} \perp c$, respectively. (The approximation for the sample geometry using Ref. 11 yielded $N_{\|} = 0.62$ and $N_{\perp} = 0.19$.) To obtain the

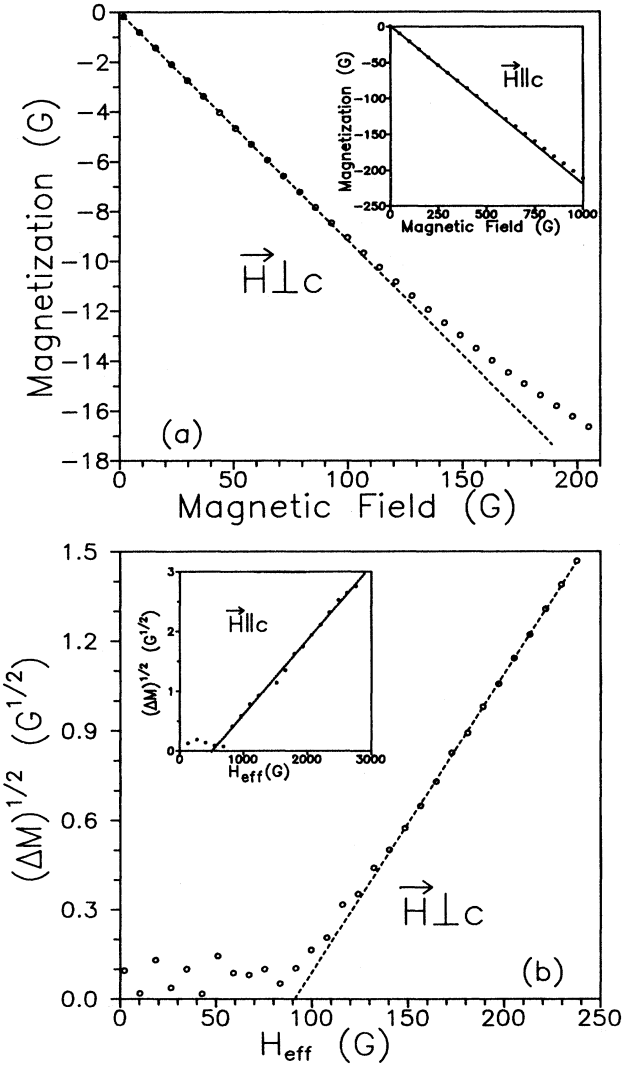

FIG. 5. Low-field magnetization of $Pb_2Sr_2(Y,Ca)Cu_3O_{8+\delta}$ at 5 K for $\mathbf{H}$ perpendicular and parallel (inset) to the c axis of the crystal. (a) M vs H. The dashed curves represent a least-squares fit to the very-low-field data. (b) $\Delta M^{1/2}$ vs the demagnetization-corrected field H_{eff}. The dashed curves represent a least-squares fit to the highest-field data.

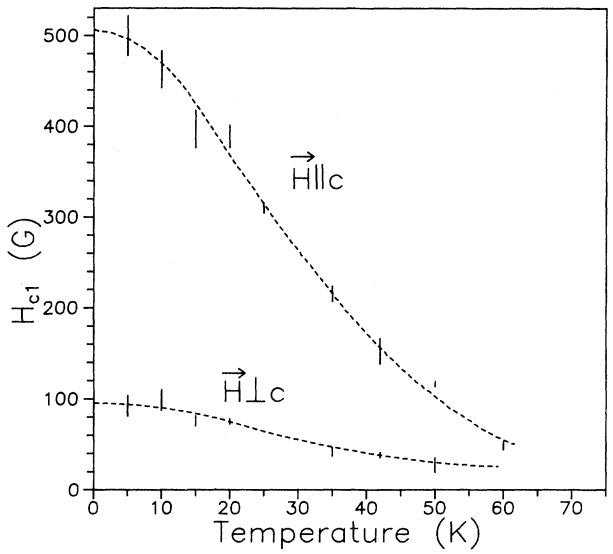

FIG. 6. Temperature dependence of the lower critical field for the c axis of the crystal oriented perpendicular ($H_{c1}^{\perp}$) and parallel ($H_{c1}^{\parallel}$) to the field direction. The dashed curves serve as a guide to the eye. These results yield estimates for the zero-temperature critical fields of 95±10 and 505±20 G for $H_{c1}^{\perp}(0)$ and $H_{c1}^{\parallel}(0)$, respectively, and an anisotropy ratio of $H_{c1}^{\parallel}(0)/H_{c1}^{\perp}(0)\approx 5$.

effective field experienced by the sample, the H axis of Fig. 5(a) should thus be multiplied by $1/1-N$. Figure 5(b) shows $(\Delta M)^{1/2}$ versus the demagnetization corrected field H_{eff} for the two crystal orientations. Note that the expected behavior is observed; $(\Delta M)^{1/2}$ is zero within experimental uncertainty (the noise is rectified so that the square root can be evaluated) up to a threshold value of H_{eff}, at which point it begins to rise. There is some rounding of the nonzero portion of the curve near H_{c1}, which Naito *et al.* attribute to the demagnetization field at the sharp corners of the crystal. They therefore suggest extracting H_{c1} by extrapolating the higher-field linear regime of the $(\Delta M)^{1/2}$-versus-H curve to the horizontal axis. Figure 6 shows the temperature dependence of the lower critical field for $\mathbf{H}\perp c$ ($H_{c1}^{\perp}$) and $\mathbf{H}\|c$ ($H_{c1}^{\parallel}$) obtained via this procedure, the uncertainty reflecting different choices for the range of points used in the least-squares fitting. The uncertainty is smaller and the threshold generally less smeared for $\mathbf{H}\perp c$, where the demagnetizing effects are less severe and the slab geometry, assumed in the analysis, is more appropriate. The values for $H_{c1}(0)$ extrapolated from these results are 95±10 and 505±20 G for $\mathbf{H}$ perpendicular and parallel to the c axis of the crystal, respectively.

V. DISCUSSION

The values obtained for H_{c1} of $Pb_2Sr_2(Y,Ca)Cu_3O_{8+\delta}$ at low temperatures are not noticeably smaller than in $YBa_2Cu_3O_{7-\delta}$, [for single-crystal $YBa_2Cu_3O_{7-\delta}$, Krusin-Elbaum *et al.*[12] estimate $H_{c1}(0)=180\pm20$ Oe for $\mathbf{H}\perp c$ and 530±50 Oe for $\mathbf{H}\|c$, while Scheidt *et al.*[6] find, respectively, 113±30 and 340±50 G for oriented powder samples]. The problem then remains of reconciling the *ab*-plane penetration depth determined for $Pb_2Sr_2(Y,Ca)Cu_3O_{8+\delta}$ (which is close to twice that of $YBa_2Cu_3O_{7-\delta}$) with a value for $H_{c1}(0)$ that is comparable to that of $YBa_2Cu_3O_{7-\delta}$. One possibility is that there is an inherent problem with the method used to extract $\lambda_{ab}(T)$. This, however, seems unlikely since Mitra *et al.* have obtained, using this method, reasonable values of $\lambda_{ab}(0)$ for polycrystalline (Y,Gd)$Ba_2Cu_3O_7$, and grain-aligned $YBa_2Cu_3O_{7-\delta}$, while Schilling, Hulliger, and Ott,[13] maintaining that no exact knowledge of the value of the anisotropy parameter is required provided $\gamma\geq 5$, extracted an equally credible value of $\lambda_{ab}=1390$ Å for polycrystalline $YBa_2Cu_3O_{7-\delta}$. In addition, we have taken the magnetization data presented by Welp *et al.*[14] for high-quality $YBa_2Cu_3O_{7-\delta}$ crystals and analyzed it according to the procedure in question. With the limited data set available [Welp *et al.* show the temperature dependence of $M_{\|c}$ for four magnetic field strengths which dictates that each $M(\ln H)$ curve be constructed from only three or four points depending on the temperature], we find good agreement with the expected trends of the method and a convincing estimate of 1100 Å for $\lambda_{ab}(0)$ based on a fit to clean-limit BCS behavior.

There are, however, some conceivable explanations for the comparatively larger value of the penetration depth in this material. One possibility is that the carrier density is intrinsically lower in this material. Preliminary *ab*-plane far-infrared reflectance measurements of these $Pb_2Sr_2(Y,Ca)Cu_3O_{8+\delta}$ crystals seem to support this view in that the plasma frequency ω_p, which is related to the carrier density n by $\omega_p^2=4\pi ne^2/m$, appears to be much lower in these materials. Here m and e refer to the effective mass and charge of the carriers, respectively. The penetration depth can be obtained from the plasma frequency using $\lambda=1/2\pi\omega_p$, where ω_p is the cm^{-1}.

It is also well known that the penetration depth can be enhanced over the London value λ^L as a result of disorder when the mean free path l is not large in comparison to the coherence length ξ. However, the *ab*-plane coherence length in these materials is already very small (approximately 15 Å), implying that the mean free path would have to be of the order of a few lattice spacings if a disorder correction were to be important. $YBa_2Cu_3O_{7-\delta}$, for instance, has been found to be well within the clean limit where $l\gg\xi$.[15] Kamarás *et al.* find from a study of the temperature dependence of the far-infrared reflectance of $YBa_2Cu_3O_{7-\delta}$ that at 100 K the scattering lifetime τ of the Drude carriers is 5.3×10^{-14} s, which, using a Fermi velocity vF of 3×10^7 cm/s, gives a mean free path of $l=160$ Å. The scattering rate is related to the dc resistivity ρ according to $\tau=m/ne^2\rho$. The normal-state dc resistivity of $Pb_2Sr_2(Y,Ca)Cu_3O_{8+\delta}$ is roughly an order of magnitude larger than in high-quality $YBa_2Cu_3O_{7-\delta}$ samples just above T_c. This would imply, assuming a similar Fermi velocity and carrier density (which, as discussed above, may not be entirely valid), that the mean free path in $Pb_2Sr_2(Y,Ca)Cu_3O_{8+\delta}$ is approximately an order of magnitude smaller than in

$YBa_2Cu_3O_{7-\delta}$, making its size comparable to that of the coherence length. That disorder may be playing a role in enhancing the penetration depth in this material can also be inferred from the fact that $Pb_2Sr_2(Y,Ca)Cu_3O_{8+\delta}$ has a residual resistivity of approximately 10% of the value of the resistivity at 300 K,[3] in contrast to high-quality $YBa_2Cu_3O_{7-\delta}$ samples where it is essentially zero. The residual resistivity is defined here as the value that the resistivity would have if the high-temperature linear behavior is extrapolated to zero temperature. In order to estimate the extent of the enhancement, we make use of the well-known expression, valid near T_c,[4]

$$\lambda(T)=\lambda^L(T)\left[1+0.75\frac{\xi}{l}\right]^{1/2}. \tag{7}$$

With $\xi_{ab}/l\approx 1$, we find $\lambda_{ab}(T)/\lambda_{ab}^L(T)=1.3$ or roughly a 30% enhancement for the *ab*-plane penetration depth (this value should be taken as an upper limit). Since, in the cuprate oxide superconductors, the coherence length along the *c* direction, ξ_c, is smaller by roughly a factor of 5 than that within the *ab* plane, the disorder correction to λ_c is ostensibly less significant. Using $\xi_c/l\approx\frac{1}{5}$, we find $\lambda_c(T)/\lambda_c^L(T)=1.07$, where $\lambda_c^L(T)$ is the London value for the penetration depth along the *c* axis. To be consistent these disorder corrections should also be taken into consideration when evaluating the effective-mass anisotropy parameter. Using these estimates, we find $\gamma^L=\lambda_c^L/\lambda_{ab}^L=1.2\gamma$, where γ is the value found for the anisotropy parameter in Sec. III (i.e., $\gamma=2.5$). The disorder-corrected value of the effective-mass anisotropy parameter would then be $\gamma^L=3$. Note that it has been assumed that the mean free path in the *c* direction, l_c, is similar to that within the *ab* plane, l_{ab}. However, l_c is likely to be smaller than l_{ab}, which would increase the *c*-axis disorder correction to the penetration depth and decrease γ^L.

What could be the source of this additional disorder in $Pb_2Sr_2(Y,Ca)Cu_3O_{8+\delta}$? One possibility is inhomogeneity in the Y,Ca distribution within the crystal. Electron probe microanalysis, however, suggests that this is not the case.[16] What is more likely is oxygen disorder. This could arise as a result of random occupation of the oxygen sites in the CuO_δ layer located between the two PbO layers. It is known that δ in polycrystalline $Pb_2Sr_2(Y,Ca)Cu_3O_{8+\delta}$ can take on values ranging from 0 (no oxygen occupation of this layer) to 2 (full oxygen occupation).[2] An accurate crystal-structure determination which includes the oxygen sites is planned using single-crystal neutron diffraction, but has not yet been performed. A rough estimate of the oxygen content of our crystals via TGA yielded $\delta=0.5$.[3] This implies that there is excess oxygen present in this Cu layer, which could give rise to disorder. Oxygen disorder can also be expected in the PbO layers as a result of the presence of the lone pair of Pb^{2+}. This unbonded pair of electrons is highly electronegative, which will cause neighboring oxygen atoms to shift their positions in order to reduce the Coulomb repulsion. A neuton-powder-diffraction experiment performed by Cava *et al.* shows evidence for such oxygen disordering in this layer.[17]

The range of values determined for $H_{c1}(0)$ of $YBa_2Cu_3O_{7-\delta}$ is still in general much wider than that for $\lambda_{ab}(0)$. If we use the more or less representative values of 1500 and 15 Å for the in-plane penetration depth and coherence length of $YBa_2Cu_3O_{7-\delta}$, respectively, we calculate, using Eq. (2) a value for $H_{c1}^{\parallel}(0)$ of 375 G, which is in reasonable agreement (within a factor of 2) with most measured values. If we make the same calculation for $Pb_2Sr_2(Y,Ca)Cu_3O_{8+\delta}$, we find using 2575 Å for $\lambda_{ab}(0)$ and 15 Å for ξ that $H_{c1}^{\parallel}(0)$ is 140 G. Using $\lambda_{ab}(0)=1800$ Å (which is the London penetration depth corresponding to a 30% disorder-enhanced penetration depth of 2575 Å, we find a value of 270 G for the zero-temperature lower critical field. This value is still smaller than the measured value of 500 G, although within a factor of 2, typical of the extent of the agreement for $YBa_2Cu_3O_{7-\delta}$.

The source of this discrepancy probably lies more with the determination of the lower critical field than with the penetration depth. A major contributor of error to the experimentally determined value of the lower critical field is the geometry of the sample. This is important for two reasons. First, sample geometry dictates the demagnetization factor that must be used in order to extract the actual value of the lower critical field from the measured field at which the first onset of flux penetration is observed. In general, the demagnetization factor is not a constant for a given sample geometry and field orientation, as we have assumed in our analysis. Since the demagnetization correction for the $\mathbf{H}\|c$ orientation of the sample is large, a small error in the determination of N can lead to considerable changes in the derived magnitude of $H_{c1}^{\parallel}$. Second, the sample morphology determines the relative importance of processes such as surface pinning which can inhibit the entry of flux until fields larger than the lower critical field predicted by the Bean model wherein only internal flux pinning is considered. The crystals of $Pb_2Sr_2(Y,Ca)Cu_3O_{8+\delta}$ are in general more cubiclike in their growth habit than crystals of the other materials. The more oblatelike shape of the $Pb_2Sr_2(Y,Ca)Cu_3O_{8+\delta}$ crystals, indicated as well by the magnitude of the experimentally derived demagnetization factors, could imply a comparatively greater contribution by surface pinning. The relative importance of the surface pinning should increase as the temperature is lowered, providing a possible explanation for the unusual temperature dependence of the in-plane lower critical field $H_{c1}^{\parallel}$ shown in Fig. 6.

The fact that the magnitude of the zero-temperature in-plane lower critical field appears to be too large is most likely caused by a combination of the effects discussed: surface pinning, uncertainty in the value of the demagnetization correction, and the questionable appropriateness of the slab geometry (utilized in the analysis of H_{c1}) for this sample orientation. In contrast, for the penetration depth no explicit sample geometry is assumed in the analysis, and because the data are obtained at intermediate fields, demagnetization corrections are negligible.

Returning finally to the subject of the extent of the anisotropy in this system, we note that the experimentally determined anisotropy parameter is smaller than the value of 5 typically quoted for $YBa_2Cu_3O_{7-\delta}$, although it

is comparable to the value of $\gamma=2.8$ found by Thompson *et al.*[18] for magnetically oriented $Tl_2Ba_2Ca_2Cu_3O_{10}$ via this same method. That the anisotropy in $Pb_2Sr_2(Y,Ca)Cu_3O_{8+\delta}$ is close to that in $Tl_2Ba_2Ca_2Cu_3O_{10}$ is not surprising since the distance between successive CuO plane bilayers is similar in the two materials [11.5 Å for $Tl_2Ba_2Ca_2Cu_3O_{10}$ compared with 12.3 Å for $Pb_2Sr_2(Y,Ca)Cu_3O_{8+\delta}$]. Unfortunately, no values for γ have been obtained for $YBa_2Cu_3O_{7-\delta}$, using the method in the form discussed herein, making meaningful comparisons difficult. However, Touminen *et al.*[19] have made use of Kogan's more general theory and extended the data-analysis procedure to incorporate the angular dependence of the magnetization. Their method involves simultaneously measuring the transverse and longitudinal components of the magnetization as a function of the angle that the c axis of the crystal makes with the direction of the applied field and then fitting the angular dependence of the ratio of transverse to longitudinal magnetization to the predictions of Kogan's theory to extract the anisotropic mass ratio. For single-crystal $YBa_2Cu_3O_{7-\delta}$ and $Bi_2Sr_2CaCu_2O_8$, they found values for γ of 5.5 and 16.7, respectively. As a means of comparison with the method used in our investigation, Touminen *et al.* also determined the anisotropy parameter for $Bi_2Sr_2CaCu_2O_8$ at 70 K by measuring the field dependence of the longitudinal magnetization only for $\mathbf{H}\perp c$ and $\mathbf{H}\parallel c$ and applying the analysis in question, i.e.,

$$\gamma=\frac{dM_{\perp c}}{d\ln H}\Big/\frac{dM_{\parallel c}}{d\ln H}\ ,$$

yielding a much smaller value of 8.9. Touminen *et al.* cite two possible reasons for the discrepancy: that, as a result of the highly anisotropic nature of the high T_c materials precise alignment is absolutely essential for the method we have utilized, since any misalignment, especially for $\mathbf{H}\perp c$, will have a substantial effect on the measured magnetization [see Eq. (2) of Ref. 19], and second, that it may be an indication that a strictly three-dimensional theory is inapplicable since a system displaying two-dimensional character within planes which are separated by essentially insulating layers would have Abrikosov-like vortices for $\mathbf{H}\parallel c$, while those for $\mathbf{H}\perp c$ would be Josephson-like. It nevertheless appears that the anisotropy in $Pb_2Sr_2(Y,Ca)Cu_3O_{8+\delta}$ is, as has been shown to be for $YBa_2Cu_3O_{7-\delta}$ and $Tl_2Ba_2Ca_2Cu_3O_{10}$ smaller than that in $Bi_2Sr_2CaCu_2O_8$.

The study of the anisotropic lower critical field can also give an indication of the extent of the anisotropy in $Pb_2Sr_2(Y,Ca)Cu_3O_{8+\delta}$. Based on the results obtained, one might conclude that, as expected, as a result of the larger interlayer spacing, the anisotropy in this system is greater than in $YBa_2Cu_3O_{7-\delta}$. Although Krusin-Elbaum *et al.* and Scheidt *et al.* disagree somewhat on the absolute values of the lower critical fields, their anisotropy ratio $H_{c1}^{\parallel}(0)/H_{c1}\perp(0)$ is almost identically equal to 3, while for $Pb_2Sr_2(Y,Ca)Cu_3O_{8+\delta}$ this study yields a value of approximately 5. We caution, however, that, as discussed above, this should be regarded as an upper limit as a result of uncertainty in determining the absolute magnitude of, in particular, the in-plane H_{c1}.

VI. CONCLUSIONS

In summary, using low- and intermediate-field magnetization measurements, we have determined the temperature dependence of the anisotropic magnetic penetration depth and lower critical field of single-crystal $Pb_2Sr_2(Y,Ca)Cu_3O_{8+\delta}$. The temperature dependence of λ_{ab} in the vicinity of T_c was found to follow BCS-like behavior, from which an estimate of 2575 Å for $\lambda_{ab}(0)$ was obtained. The effective-mass anisotropy parameter $\gamma=(m_c/m_{ab})^{1/2}$ was determined to be 2.5, which, together with the former result, gives $\lambda_c(0)=6425$ Å. We suggest that the enhanced value of λ_{ab} in this material over that of $YBa_2Cu_3O_{7-\delta}$ may be due to a lower intrinsic carrier concentration or, in part, due to oxygen disorder in the PbO-CuO_δ-PbO layer sequence which distinguishes $Pb_2Sr_2(Y,Ca)Cu_3O_{8+\delta}$ structurally from the other materials. The comparatively larger value for $\lambda_{ab}(0)$ in $Pb_2Sr_2(Y,Ca)Cu_3O_{8+\delta}$ should imply a smaller value for $H_{c1}^{\parallel}(0)$. The experimental estimates for the zero-temperature lower critical fields of 95 ± 10 and 505 ± 20 G for $\mathbf{H}\perp c$ and $\mathbf{H}\parallel c$, respectively, are, however, not noticeably smaller than those for $YBa_2Cu_3O_{7-\delta}$. We feel that the source of the discrepancy lies mainly in the determination of $H_{c1}^{\parallel}$, where difficulties such as surface pinning and imperfect demagnetization and model geometries can cause large uncertainty in the value obtained. The result quoted should therefore be regarded as an upper limit.

ACKNOWLEDGMENTS

We thank E. J. Nicol for providing the theoretical $\lambda(0)/\lambda(T)$ curves and for helpful discussions. This work was supported by the Natural Science and Engineering Research Council of Canada (NSERC), including infrastructure support for the Institute for Materials Research.

[1]S. Martin, A. T. Fiory, R. M. Fleming, L. F. Schneemeyer, and J. V. Waszczak, Phys. Rev. Lett. **60**, 2194 (1988); D. E. Farrell, S. Bonham, J. Foster, Y. C. Chang, P. Z. Jiang, K. G. Vandervoort, D. J. Lam, and V. G. Kogan, *ibid.* **63**, 782 (1989); T. T. M. Palstra, B. Batlogg, L. F. Schneemeyer, R. B. van Dover, and J. V. Waszczak, Phys. Rev. B **38**, 5102 (1988); T. T. M. Palstra, B. Batlogg, R. B. van Dover, L. F. Schneemeyer, and J. V. Waszczak, *ibid.* **41**, 6621 (1990).

[2]R. J. Cava, B. Batlogg, J. J. Krajewski, L. W. Rupp, L. F. Schneemeyer, T. Siegrist, R. B. van Dover, P. Marsh, W. F. Peck, Jr., P. K. Gallagher, S. H. Glarum, J. H. Marshall, R. C. Farrow, J. V. Waszczak, R. Hull, and P. Trevor, Nature **336**, 211 (1988).

[3]J. S. Xue, M. Reedyk, Y. P. Lin, C. V. Stager, and J. E. Greedan, Physica C **166**, 29 (1990).

[4]M. Tinkham, *Introduction to Superconductivity* (Krieger, Mala-

bar, FL, 1980); D. Saint-James, G. Sarma, and E. J. Thomas, *Type II Superconductivity* (Pergamon, Oxford, 1969).
[5]V. G. Kogan, M. M. Fang, and S. Mitra, Phys. Rev. B **38**, 11 958 (1988).
[6]L. Krusin-Elbaum, R. L. Greene, F. Holtzberg, A. P. Malozemoff, and Y. Yeshurun, Phys. Rev. Lett. **62**, 217 (1989); E. W. Scheidt, C. Hucho, K. Lüders, and V. Müller, Solid State Commun. **71**, 505 (1989); B. Pümpin, H. Keller, W. Kündig, W. Odermatt, I. M. Savić, J. W. Schneider, H. Simmler, P. Zimmermann, E. Kaldis, S. Rusiecki, Y. Maeno, and C. Rossel, Phys. Rev. B **42**, 8019 (1990).
[7]C. M. Foster, K. F. Voss, T. W. Hagler, D. Mihailović, A. J. Heeger, M. M. Eddy, W. L. Olson, and E. J. Smith, Solid State Commun. **76**, 651 (1990).
[8]S. Mitra, J. H. Cho, W. C. Lee, D. C. Johnston, and V. G. Kogan, Phys. Rev. B **40**, 2674 (1989).
[9]M. Naito, A. Matsuda, K. Kitazawa, S. Kambe, I. Tanaka, and H. Kojima, Phys. Rev. B **41**, 4823 (1990).
[10]C. P. Bean, Rev. Mod. Phys. **36**, 31 (1964).
[11]G. W. Crabtree, Phys. Rev. B **16**, 1117 (1977).
[12]L. Krusin-Elbaum, A. P. Malozemoff, Y. Yeshurun, D. C. Cronemeyer, and F. Holtzberg, Phys. Rev. B **39**, 2936 (1989).
[13]A. Schilling, F. Hulliger, and H. R. Ott, Physica C **168**, 272 (1990).
[14]U. Welp. W. K. Kwok, G. W. Crabtree, K. G. Vandervoort, and J. Z. Liu, Phys. Rev. Lett. **62**, 1908 (1989).
[15]K. Kamarás, S. L. Herr, C. D. Porter, N. Tache, D. B. Tanner, S. Etemad, T. Venkatesan, E. Chase, A. Inam, X. D. Wu, M. S. Hegde, and B. Dutta, Phys. Rev. Lett. **64**, 84 (1990).
[16]J. S. Xue, M. Reedyk, A. Dabkowski, H. Dabkowska, J. E. Greedan, and C. H. Chen (unpublished).
[17]R. J. Cava, M. Marezio, J. J. Krajewski, W. F. Peck, Jr., A. Santoro, and F. Beech, Physica C **157**, 272 (1989).
[18]J. R. Thompson, D. K. Christen, H. A. Deeds, Y. C. Kim, J. Brynestad, S. T. Sekula, and J. Budai, Phys. Rev. B **41**, 7293 (1990).
[19]M. Tuominen, A. M. Goldman, Y. Z. Chang, and P. Z. Jiang, Phys. Rev. B **42**, 412 (1990).